Volumetric Contact Model of Ellipsoid-Plane Geometries

Peter Brown, John McPhee

Systems Design Engineering
University of Waterloo
200 University Avenue W, Waterloo, ON, Canada N2L 3G1
[pm2brown,mcphee]@uwaterloo.ca

Abstract

Contact models of conforming surfaces are difficult to model accurately and efficiently. In multibody dynamics simulations, contact models increase system equation complexity (often dramatically so) and can also introduce nonlinearities and discontinuities into the system equations, decreasing the computational efficiency. This is particularly problematic in predictive simulations, which may determine optimal performance by running a simulation thousands of times. Contact modelling is even more complicated for large conforming surfaces, where the contact cannot be simplified to a single point. An ideal contact model must find a balance between accuracy and computational efficiency. Volumetric contact modelling is explored as a computationally efficient model conforming contacts. Volumetric contact has been used previously in robotics and biomechanics contacts, but analytical contact equations have only been derived for sphere-plane contact and 2D shapes. The model presented here improves on current work by deriving analytical volumetric contact equations for ellipsoid-plane contact which can better represent the shape of some contact surfaces. Equations for the volumetric geometrical values, normal force and damping, rolling resistance, tangential friction, and spinning friction were derived. Friction is approximated using a continuous velocity-based model of friction, and the possible limitations of this are described. This model may be useful for future use in modelling conforming contacts that can be approximated as an ellipsoid contacting a plane.

Keywords: contact dynamics, volumetric contact, ellipsoid

1. Introduction

Forward dynamics simulation, or predictive simulation, is a useful tool for the predicting the performance of a multibody system. A forward dynamics model can be used in an optimisation routine with a cost function that rewards system performance in order to optimise the design of a system. Optimisation may require many simulations to converge to a solution (often thousands), so a computationally efficient multibody model is needed, as well as an accurate one.

One important aspect of some multibody models is contact modelling. Contact is difficult to model since contact forces are often nonlinear, discontinuous, and result in stiff system equations. The motivation for this research was to develop an efficient foot-ground contact model for gait simulation. The foot plantar surface is relatively large and compliant, which requires a more complex model than a surface with a small contact area.

Detailed and accurate contact models that can account for complex and conforming contacts tend to be computationally expensive (such as finite element models), making them poorly suited for optimisations [1], [2]. Simpler contact models are often based on point-contact models [3]–[5] which are computationally efficient, but are only accurate for small contact patches (not conforming surfaces). This issue can be partially alleviated by using a large number of point contacts over the contact surface [6]–[9]. Alternatively, point contact models can be modified by using contact geometry to determine the central or most important point of contact and apply the reaction forces at that point [8], [10].

A balance is needed between a simplified model that will be computationally efficient, and an accurate model. Volumetric contact shows potential as an efficient continuous contact model for large contact surfaces.

2. Volumetric Contact

Volumetric contact was first proposed by Gonthier et al. for contact in robotic manipulators [11], [12]. Volumetric contact is based on the elastic foundation model, which models the surface as a continuous collection of springs, as shown in Figure 1.

Since volumetric contact considers the pressure developed across the whole contact surface, it is more accurate than point contact models for complex and conforming geometries [13]. This also means that the pressure across the

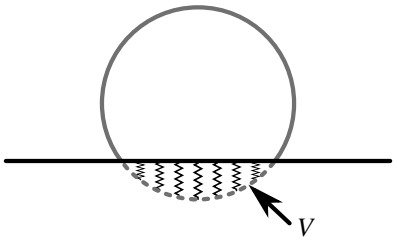

Figure 1: Volumetric contact surface interaction

contact surface can be calculated naturally with volumetric contact, unlike point contact models. The contact forces can be found as an integral of the stresses developed across the contact area. If the contact geometry is represented as simplified shapes—which is generally done for volumetric contact—the distributed forces over the contact surface can be integrated to obtain analytical equations for the equivalent forces and torques at a resultant point. This results in a set of equations much more efficient than discrete elastic foundation models, and not significantly more complex than point contact models.

For volumetric contact, if the surface stiffness is linear, integration across the contact surface reveals that the normal force is directly proportional to the volume of penetration of the two surfaces. Similarly, the centre of pressure (COP) is at the centroid of this volume of penetration, and all other contact forces (rolling resistance and friction) can be related to the volume of penetration and its properties [13], [14]. This allows for a simplified set of contact equations if the contact volume and other geometric properties have analytical solutions.

To expand on previous work, analytical equations for ellipsoid-plane volumetric contact are derived in this paper. Ellipsoids can match complex geometry more closely than spheres can, allowing for various geometries to be modelled more accurately. Previously derived equations for sphere-plane contact [13], [15]–[17] will be used as a basis for ellipsoid-plane contact, with reference to Gonthier's detailed equations of volumetric contact [14].

3. Volumetric Contact Geometrical Values

3.1. Properties of sphere-plane contact

Contact equations for a generic sphere-plane contact were used as a basis for the ellipsoid-plane equations. Let a unit sphere intersect a plane, where frame S is located at the centre of the sphere, $\vec{c}_S$ is the centroid of the volume of penetration, $\vec{p}_S$ is a point on the plane, $\hat{\mathbf{n}}_S$ is the normal of the plane (for ground contact, this vector would point upwards), and d is the depth of penetration (see Figure 2).

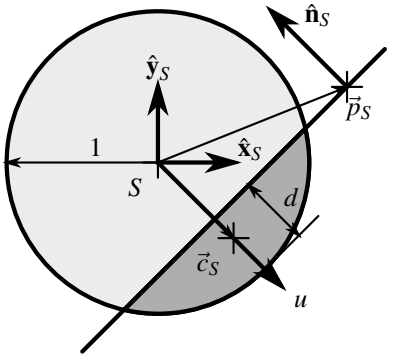

Figure 2: Sphere plane diagram

For volumetric contact, some of the properties are based on the location of an imaginary contact plane (the normal force is assumed to be perpendicular to this plane). For sphere-plane contact, the plane was treated as this contact plane, and the same will be done for ellipsoid-plane contact.

It is useful to define several properties based on the depth of penetration d:

$$d = 1 + \vec{p}_S \cdot \hat{\mathbf{n}}_S \tag{1}$$

For penetration distance d, the penetration volume can be defined as an integral of a revolution about the plane normal

axis. Let a temporary u-axis point along $-\hat{\mathbf{n}}_S$ from the centre of the sphere, such that $r^2 = 1 - u^2$. The volume of penetration is:

$$\begin{aligned} V_S &= \int_{1-d}^{1} \pi r^2 \mathrm{d}u \\ &= -\frac{1}{3}\pi d^2(d-3) \end{aligned} \tag{2}$$

Due to symmetry, the centroid must be along the u-axis.

$$\vec{c}_S = -c_S \hat{\mathbf{n}}_S \tag{3}$$

where

$$\begin{aligned} c_S &= \frac{1}{V_S}\int_{1-d}^{1} \pi r^2 u \mathrm{d}u \\ &= -\frac{3(d-2)^2}{4d-12} \end{aligned} \tag{4}$$

Another property of interest for volumetric contact is the *weighted second moment of area* (weighted by the depth of penetration). This can also be thought of as the second moment of volume of the volume of penetration, with all the volume compressed into a single plane parallel with the contact surface. The perpendicular axis theorem [18, p. 241] applies this property: the second moment of volume about the plane normal axis must be equal to the sum of the second moment of volume for two perpendicular axes lying in the plane. Due to symmetry of the sphere-plane penetration volume, the second moment of volume for any axis lying in the plane must be equal and the second moment of volume about the plane normal is twice that of an axis tangential to the plane.

The weighted second moment of area about the plane normal can be defined as:

$$\begin{aligned} J_n &= \int_{1-d}^{1} \frac{1}{2}\pi r^4 \mathrm{d}u \\ &= \frac{1}{30} d^3 \pi (3d^2 - 15d + 20) \end{aligned} \tag{5}$$

As mentioned before, the weighted second moment of area about an axis tangential to the plane would be half this amount:

$$J_t = \frac{1}{60} d^3 \pi (3d^2 - 15d + 20) \tag{6}$$

3.2. Sphere-ellipsoid conversion

To find the geometrical properties for an ellipsoid, assume that the sphere is stretched along all three axes to form an ellipsoid: by a factor of a along the x-axis, b along the y-axis, and c along the z-axis (Figure 3).

To convert the geometrical values of a sphere-plane penetration volume to that of an ellipsoid-plane penetration volume, let there be an equivalent, scaled frame E at the centre of the ellipsoid where

$$x_E = a x_S \tag{7}$$

$$y_E = b y_S \tag{8}$$

$$z_E = c z_S \tag{9}$$

Note that in Figure 3 $\hat{\mathbf{n}}_E$ is not the scaled version of $\hat{\mathbf{n}}_S$, but the normal of the scaled plane.

Then the point on the plane in frame E can be related to the same point in frame S as:

$$\vec{p}_E = \mathbf{S}\vec{p}_S \tag{10}$$

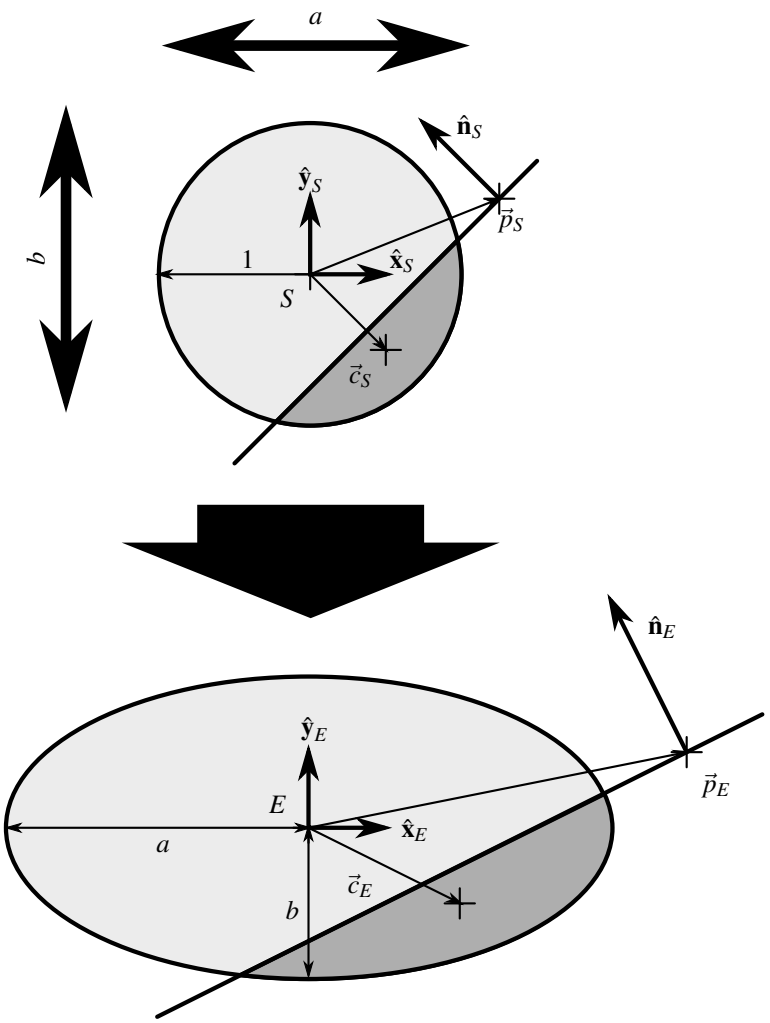

Figure 3: Sphere scaled to ellipsoid

where **S** defines a "stretch matrix" for the frame transformation:

$$\mathbf{S} = \begin{bmatrix} a & 0 & 0 \\ 0 & b & 0 \\ 0 & 0 & c \end{bmatrix} \tag{11}$$

Since the plane has been stretched, the direction of the plane normal vector would be changed by the inverse of the stretch matrix:

$$\hat{\mathbf{n}}_E = \frac{\mathbf{S}^{-1}\hat{\mathbf{n}}_S}{|\mathbf{S}^{-1}\hat{\mathbf{n}}_S|} \tag{12}$$

Similarly,

$$\hat{\mathbf{n}}_S = \frac{\mathbf{S}\hat{\mathbf{n}}_E}{|\mathbf{S}\hat{\mathbf{n}}_E|} \tag{13}$$

3.3. Penetration volume and centroid

The penetration volume for the sphere has already been defined in Equation (4). The volume may also be defined as a triple integral:

$$V_S = \iiint_V \mathrm{d}x_S \mathrm{d}y_S \mathrm{d}z_S \tag{14}$$

where V represents the volume of penetration. For the ellipsoid:

$$V_E = \iiint_V \mathrm{d}x_E \mathrm{d}y_E \mathrm{d}z_E$$

Substitute Equations (7)–(9) to relate the volume of penetration of an ellipsoid to that of a unit sphere (Equation (14)):

$$\begin{aligned} V_E &= \iiint_V a\mathrm{d}x_S b\mathrm{d}y_S c\mathrm{d}z_S \\ &= abc \iiint_V \mathrm{d}x_S \mathrm{d}y_S \mathrm{d}z_S \\ V_E &= abcV_S \end{aligned} \tag{15}$$

Thus, the volume of penetration of an ellipsoid is the scaled volume of penetration of a sphere.

Similarly, the centroid of penetration can be related using the basic definition of the centroid of volume:

$$\vec{c}_S = \frac{1}{V_S} \begin{bmatrix} \int_V x_S \mathrm{d}V_S \\ \int_V y_S \mathrm{d}V_S \\ \int_V z_S \mathrm{d}V_S \end{bmatrix} \tag{16}$$

In frame E:

$$\begin{aligned} \vec{c}_E &= \frac{1}{V_E} \begin{bmatrix} \int_V x_E \mathrm{d}V_E \\ \int_V y_E \mathrm{d}V_E \\ \int_V z_E \mathrm{d}V_E \end{bmatrix} \\ &= \frac{1}{abcV_S} \begin{bmatrix} \int_V ax_S abc \mathrm{d}V_S \\ \int_V by_S abc \mathrm{d}V_S \\ \int_V cz_S abc \mathrm{d}V_S \end{bmatrix} \\ &= \frac{1}{V_S} \begin{bmatrix} a\int_V x_S \mathrm{d}V_S \\ b\int_V y_S \mathrm{d}V_S \\ c\int_V z_S \mathrm{d}V_S \end{bmatrix} \\ \vec{c}_E &= \mathbf{S}\vec{c}_S \end{aligned} \tag{17}$$

3.4. Second moment of contact area

To determine the equivalent weighted second moment of area for an ellipse, first consider an arbitrary second moment of volume matrix:

$$\mathbf{J} = \begin{bmatrix} J_{xx} & J_{xy} & J_{xz} \\ J_{xy} & J_{yy} & J_{yz} \\ J_{xz} & J_{yz} & J_{zz} \end{bmatrix} \tag{18}$$

where:

$$J_{xx} = \iiint (y^2 + z^2)\mathrm{d}V \tag{19}$$

$$J_{yy} = \iiint (x^2 + z^2)\mathrm{d}V \tag{20}$$

$$J_{zz} = \iiint (x^2 + y^2)\mathrm{d}V \tag{21}$$

$$J_{xy} = -\iiint xy\mathrm{d}V \tag{22}$$

$$J_{xz} = -\iiint xz\mathrm{d}V \tag{23}$$

$$J_{yz} = -\iiint yz\mathrm{d}V \tag{24}$$

A property that may be noted from Equations (19)–(21) is that:

$$\iiint x^2 \mathrm{d}V = \frac{1}{2}\left(J_{yy} + J_{zz} - J_{xx}\right) \tag{25}$$

$$\iiint y^2 \mathrm{d}V = \frac{1}{2}\left(J_{xx} + J_{zz} - J_{yy}\right) \tag{26}$$

$$\iiint z^2 \mathrm{d}V = \frac{1}{2}\left(J_{xx} + J_{yy} - J_{zz}\right) \tag{27}$$

If an object with second moment of volume $\mathbf{J}$ were to be stretched, by a factor of a along the x-axis, b along the y-axis, and c along the z-axis then the new value for J_{xx} is:

$$\begin{aligned} J'_{xx} &= \iiint ((by)^2 + (cz)^2)\mathrm{d}(abcV) \\ &= (abc)\left(b^2 \iiint y^2 \mathrm{d}V + c^2 \iiint z^2 \mathrm{d}V\right) \end{aligned}$$

using Equations (26) and (27) to relate back to the elements of $\mathbf{J}$:

$$J'_{xx} = \frac{abc}{2}\left(b^2(J_{xx} + J_{zz} - J_{yy}) + c^2(J_{xx} + J_{yy} - J_{zz})\right) \tag{28}$$

Similarly

$$J'_{yy} = \frac{abc}{2}\left(a^2(J_{yy} + J_{zz} - J_{xx}) + c^2(J_{xx} + J_{yy} - J_{zz})\right) \tag{29}$$

$$J'_{zz} = \frac{abc}{2}\left(a^2(J_{yy} + J_{zz} - J_{xx}) + b^2(J_{xx} + J_{zz} - J_{yy})\right) \tag{30}$$

For the off-diagonal elements of $\mathbf{J}$:

$$J'_{xy} = a^2 b^2 c J_{xy} \tag{31}$$

$$J'_{xz} = a^2 b c^2 J_{xz} \tag{32}$$

$$J'_{yz} = a b^2 c^2 J_{yz} \tag{33}$$

Equations (28)–(33) can be used to define the transformation to the second moment of volume matrix when any volume is scaled along all the x, y, and z-axes by factors of a, b, and c, respectively. Let this transformation be defined by the function "scale" where

$$\mathbf{J}' = \mathrm{scale}(\mathbf{J}, a, b, c) \tag{34}$$

In order to transform the weighted second moment of area of the sphere to that of the ellipsoid, two more coordinate frames will be defined at the penetration volume centroid. Assume that there is a known coordinate frame for the plane in contact with the ellipsoid in frame E (frame PE), where the z-axis is perpendicular to the plane (parallel with $\hat{\mathbf{n}}_E$) (see Figure 4).

Additionally, let there be a frame at the centroid of the sphere-plane volume, PS, with the z-axis parallel with $\hat{\mathbf{n}}_S$ and the x-axis along the transformed $\vec{x}_{PE}$ axis:

$$\hat{\mathbf{x}}_{PS} = \frac{\mathbf{S}^{-1}\hat{\mathbf{x}}_{PE}}{|\mathbf{S}^{-1}\hat{\mathbf{x}}_{PE}|} \tag{35}$$

The y-axis is defined by the cross-product of the z- and x-axis.

With the coordinate frames fully defined, also let $\mathbf{R}_{PE}$ be the rotation matrix from frame PE to E, and $\mathbf{R}_{PS}$ from PS to S.

The weighted second moment of area for a sphere-plane contact has been defined for the normal and tangential axes (Equations (5) and (6)). This lines up with frame PS, and can be represented in a matrix:

$$\mathbf{J}_{PS} = \begin{bmatrix} J_t & 0 & 0 \\ 0 & J_t & 0 \\ 0 & 0 & J_n \end{bmatrix} \tag{36}$$

In order to transform this from frame PS to PE, the equivalent will be found in frame S (by finding the rotation), then scaled to frame E, and then rotated to frame PE:

$$\mathbf{J}_{PE} = \mathbf{R}_{PE}^T \,\mathrm{scale}\left(\mathbf{R}_{PS}\,\mathbf{J}_{PS}\,\mathbf{R}_{PS}^T, a, b, c\right)\mathbf{R}_{PE} \tag{37}$$

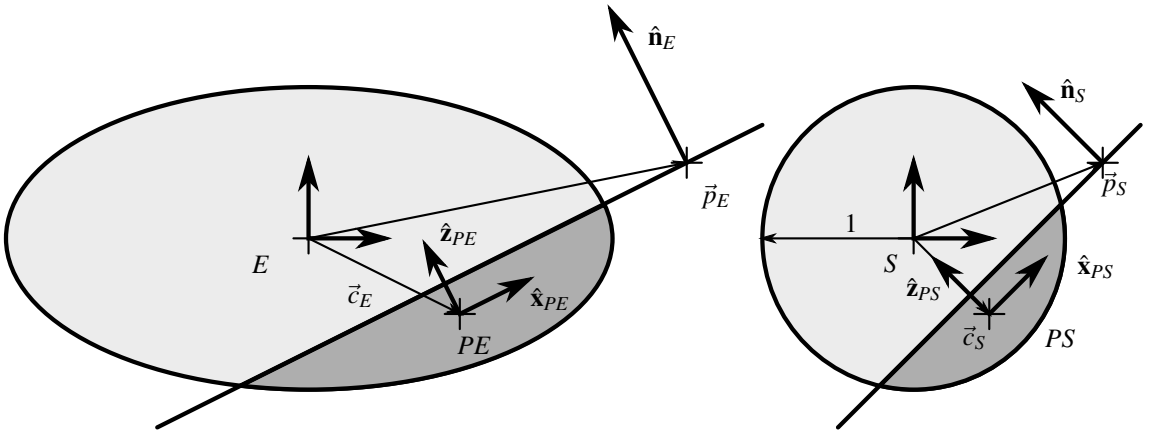

Figure 4: Sphere and ellipsoid contact with vectors for frame at centroid

3.5. Relative velocity

The relative velocity of the two bodies at the penetration volume centroid is also of interest for volumetric contact. See Figure 5 for frame and velocity definitions.

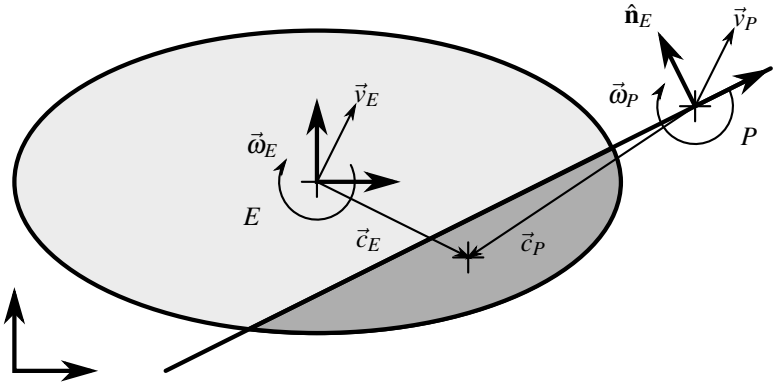

Figure 5: Sphere and ellipsoid contact relative velocity

The relative velocity of the two bodies at the centroid is:

$$\vec{v}_c = \vec{v}_E + \vec{\omega}_E \times \vec{c}_E - (\vec{v}_P + \vec{\omega}_P \times \vec{c}_P) \tag{38}$$

which can be divided into normal and tangential components based on the plane normal $\hat{\mathbf{n}}_E$:

$$\vec{v}_{cn} = (\vec{v}_c \cdot \hat{\mathbf{n}}_E)\hat{\mathbf{n}}_E \tag{39}$$

$$\vec{v}_{ct} = \vec{v}_c - \vec{v}_{cn} \tag{40}$$

The relative rotational velocity between the two bodies is:

$$\vec{\omega}_c = \vec{\omega}_E - \vec{\omega}_P \tag{41}$$

with components:

$$\vec{\omega}_{cn} = (\vec{\omega}_c \cdot \hat{\mathbf{n}}_E)\hat{\mathbf{n}}_E \tag{42}$$

$$\vec{\omega}_{ct} = \vec{\omega}_c - \vec{\omega}_{cn} \tag{43}$$

3.6. Equation manipulation

The equations for the geometrical values of volumetric contact were expanded and simplified by using symbolic computing software Maple (2016. Maplesoft, Waterloo, ON, Canada). Due to the length and complexity of the equations, they will not be given here.

It was noted that the equations for the ellipsoid-plane model were significantly more complex than the sphere-plane contact model on which it was based. In the authors' opinion, it is likely that the equations for more complex shapes, especially those with less symmetry, will be even more complex or infeasible to determine analytically.

4. Contact Forces and Moments

4.1. Normal force

From Gonthier's derivations [14], the normal force for volumetric contact is:

$$\vec{F}_n = k_V V \left(1 + a_V |\vec{v}_{cn}|\right) \hat{\mathbf{n}}_E \tag{44}$$

where k_V is the volumetric stiffness and a_V is the damping coefficient. The other values (volume of penetration V and relative normal velocity $\vec{v}_{cn}$) were defined or derived in Section 3.

4.2. Rolling resistance moment

Rolling resistance for volumetric contact is given as [14]:

$$\vec{\tau}_r = k_V a_V \mathbf{J} \vec{\omega}_{ct} \tag{45}$$

where $\mathbf{J}$ is the weighted second moment of area ($\mathbf{J}_{PE}$ in Section 3) and $\vec{\omega}_{ct}$ is the relative tangential angular velocity.

4.3. Tangential friction force

Gonthier approximated tangential friction as follows [14]:

$$\vec{F}_t = F_n \mu \vec{v}_{ct} \tag{46}$$

where μ is a coefficient of friction, F_n the magnitude of the normal force, and $\vec{v}_{ct}$ the tangential relative velocity at the centroid.

To obtain a friction model that more closely matched dry friction, a continuous velocity-based model was used [19]. Incorporating that friction equation into Equation (46) resulted in the following model:

$$\vec{F}_t = F_n \mu(|\vec{v}_{ct}|) \frac{\vec{v}_{ct}}{|\vec{v}_{ct}|} \tag{47}$$

where

$$\mu(v) = \mu_d \tanh\left(4\frac{v}{v_t}\right) + (\mu_s - \mu_d) \frac{\frac{v}{v_t}}{\left(\frac{1}{4}\left(\frac{v}{v_t}\right)^2 + \frac{3}{4}\right)^2} \tag{48}$$

where μ_d is the dynamic coefficient of friction, μ_s the static coefficient of friction, and v_t the transition velocity.

4.4. Spinning friction moment

Gonthier's approximation for spinning friction is:

$$\vec{\tau}_s = \mu \frac{F_n}{V} \mathbf{J} \vec{\omega}_{cn} \tag{49}$$

Similar to tangential friction, this was adapted using the same friction model:

$$\vec{\tau}_s = \frac{F_n}{V} \mu(|\vec{\omega}_{cn}|) \mathbf{J} \frac{\vec{\omega}_{cn}}{|\vec{\omega}_{cn}|} \tag{50}$$

where

$$\mu(\omega) = \mu_d \tanh\left(4\frac{\omega}{\omega_t}\right) + (\mu_s - \mu_d) \frac{\frac{\omega}{\omega_t}}{\left(\frac{1}{4}\left(\frac{\omega}{\omega_t}\right)^2 + \frac{3}{4}\right)^2} \tag{51}$$

where ω_t is the transition angular velocity.

4.5. Accuracy of friction equations

Note that these friction equations are an adaptation of an averaged integral. Due to simplifications, this friction model may not be accurate in all cases, such as when contact has a mixture of sticking and slipping or when a large amount of spinning is present. Also, the model does not have exact stiction (since it uses a velocity-based friction model) and does not capture the Contensou effect (since the tangential friction and spinning friction equations are decoupled).

The model should be a good approximation for foot-ground contact (the motivation behind this study) since it has a relatively short contact time, low surface velocities, and little spinning. These simplifications may be a concern in other applications where more spinning and slipping is present, especially if the value of friction is of interest.

5. Conclusion

Analytical equations for volumetric contact between an ellipsoid and a plane were derived and presented, based on the equations for sphere-plane contact.

The friction model was adjusted from Gonthier's proposed equations to match more closely with Coulomb friction. In order to keep the equations analytical, the friction model was an approximation that cannot capture all effects, such as perfect sticking or the Contensou effect.

These equations may be useful for modelling conforming contacts, especially contacts with geometry similar to an ellipsoid.

Acknowledgments

This research was funded by the Natural Sciences and Engineering Research Council of Canada and the Canada Research Chairs program.

References

[1] A. Pérez-González, C. Fenollosa-Esteve, J. L. Sancho-Bru, F. T. Sánchez-Marín, M. Vergara, and P. J. Rodríguez-Cervantes, "A modified elastic foundation contact model for application in 3D models of the prosthetic knee," *Medical Engineering and Physics*, vol. 30, no. 3, pp. 387–398, 2008.

[2] J. P. Halloran, M. Ackermann, A. Erdemir, and A. J. van den Bogert, "Concurrent musculoskeletal dynamics and finite element analysis predicts altered gait patterns to reduce foot tissue loading," *Journal of Biomechanics*, vol. 43, no. 14, pp. 2810–2815, 2010.

[3] P. Flores, M. Machado, M. T. Silva, and J. M. Martins, "On the continuous contact force models for soft materials in multibody dynamics," *Multibody System Dynamics*, vol. 25, no. 3, pp. 357–375, 2011.

[4] J. M. Font-Llagunes, A. Barjau, R. Pàmies-Vilà, and J. Kövecses, "Dynamic analysis of impact in swing-through crutch gait using impulsive and continuous contact models," *Multibody System Dynamics*, vol. 28, no. 3, pp. 257–282, 2012.

[5] S. Hu and X. Guo, "A dissipative contact force model for impact analysis in multibody dynamics," *Multibody System Dynamics*, vol. 35, no. 2, pp. 131–151, 2015.

[6] F. C. Anderson and M. G. Pandy, "Dynamic optimization of human walking," *ASME Journal of Biomechanical Engineering*, vol. 123, no. 5, pp. 381–390, 2001.

[7] D. Dopico, A. Luaces, M. Gonzalez, and J. Cuadrado, "Dealing with multiple contacts in a human-in-the-loop application," *Multibody System Dynamics*, vol. 25, no. 2, pp. 167–183, 2011.

[8] D. S. Lopes, R. R. Neptune, J. A. Ambrósio, and M. T. Silva, "A superellipsoid-plane model for simulating foot-ground contact during human gait," *Computer Methods in Biomechanics and Biomedical Engineering*, pp. 1–10, 2015.

[9] J. N. Jackson, C. J. Hass, and B. J. Fregly, "Development of a subject-specific foot-ground contact model for walking," *ASME Journal of Biomechanical Engineering*, vol. 138, no. 9, 091002:1–12, 2016.

[10] M. Millard and A. Kecskeméthy, "A 3D foot-ground model using disk contacts," in *The 3rd Joint International Conference on Multibody System Dynamics & The 7th Asian Conference on Multibody Dynamics*, Busan, Korea, 2014.

[11] Y. Gonthier, J. McPhee, C. Lange, and J.-C. Piedbœuf, "A contact modeling method based on volumetric properties," in *ASME IDETC*, Long Beach, California, USA, 2005, pp. 477–486.

[12] Y. Gonthier, C. Lange, and J. McPhee, "A volumetric contact model implemented using polynomial geometry," in *Multibody Dynamics 2009, ECCOMAS Thematic Conference, Warsaw, Poland*, 2009.

[13] M. Boos and J. McPhee, "Volumetric modeling and experimental validation of normal contact dynamic forces," *ASME Journal of Computational and Nonlinear Dynamics*, vol. 8, no. 2, 021006:1–8, 2013.

[14] Y. Gonthier, "Contact dynamics modelling for robotic task simulation," PhD Thesis, University of Waterloo, 2007.

[15] M. Millard, J. McPhee, and E. Kubica, "Multi-step forward dynamic gait simulation," in *Multibody Dynamics: Computational Methods and Applications*, C. L. Bottasso, Ed., Dordrecht: Springer Netherlands, 2009, pp. 25–43.

[16] M. Sharif Shourijeh and J. McPhee, "Forward dynamic optimization of human gait simulations: A global parameterization approach," *ASME Journal of Computational and Nonlinear Dynamics*, vol. 9, no. 3, 031018:1–11, 2014.

[17] M. S. Shourijeh and J. McPhee, "Foot-ground contact modeling within human gait simulations: From Kelvin-Voigt to hyper-volumetric models," *Multibody System Dynamics*, vol. 35, no. 4, pp. 393–407, 2015.

[18] P. A. Tipler, *Physics for scientists and engineers*, 3rd ed. New York, NY: Worth Publishers, 1991.

[19] P. Brown and J. McPhee, "A continuous velocity-based friction model for dynamics and control with physically meaningful parameters," *ASME Journal of Computational and Nonlinear Dynamics*, vol. 11, no. 5, 054502:1–6, 2016.